

# TEMPERATURE DEPENDENCE OF IRRADIATION-INDUCED U-MO-AL INTERDIFFUSION

B. Ye, G.L. Hofman, A. Bergeron, Y. Miao  
*Argonne National Laboratory*  
9700 South Cass Ave, Argonne, IL 60439 USA

D. Salvato, A. Leenaers, S. Van den Berghe  
*Nuclear Material Science Institute, SCK·CEN*  
Boeretang 200, 2400 Mol, Belgium

J. Shi, H. Breitzkreutz  
*Forschungs-Neutronenquelle Heinz Maier-Leibnitz (FRM II), Technische Universität München*  
Lichtenbergstr. 1, 85747 Garching, Germany

## ABSTRACT

In order to comprehend the transition of the growth rate of interdiffusion layers (IL) at the interfaces of U-7Mo particles and the Al matrix in in-pile-irradiated U-Mo/Al dispersion fuel, the temperature effect on IL growth was studied. The variation of active energy in different temperature regimes is responsible for the change of IL growth rate. A new IL growth correlation (Correlation II) was therefore formulated by incorporating the transition temperature. The transition temperature and activation energy for U-Mo-Al interdiffusion in different U-Mo/Al dispersion fuel systems were fitted based on in-pile irradiation data using the DART-2D code. In addition, the effective contact surface area between U-Mo particles and the Al matrix is also considered. Sensitivity study was performed to evaluate how much the change of each parameter affects IL growth and fuel meat swelling.

## 1. Introduction

In-pile irradiation results [1]-[3] of full-size U-Mo/Al dispersion fuel plates showed that the growth rate of U-Mo-Al interdiffusion layers (IL) at the interfaces of U-Mo particles and the Al matrix has a transition at a threshold fission rate: low to moderate IL growth at the locations where the fission rate was lower than the threshold and accelerated growth with a small activation energy at the locations where the fission rate was above the threshold. The observed IL growth behavior was described with a correlation (designated as Correlation I) that is expressed as a modified Arrhenius equation multiplied by a temperature-dependent sigmoidal function transiting around a threshold fission rate in a previous study [4], as expressed in Eq. (1):

$$\Delta Y^2 = 2.6 \times 10^{-16} (\dot{f})^{0.5} \cdot \Delta t \cdot \exp\left(-\frac{7700}{R \cdot T}\right) \cdot F_{reduction} \quad (1)$$

where  $\Delta Y$  is the incremental IL thickness within a time step in cm,  $\dot{f}$  is the fission rate in fissions/(cm<sup>3</sup>·s),  $\Delta t$  is the time interval in s,  $R$  is the universal gas constant given by  $R = 1.987$

cal/K/mol,  $T$  is the fuel meat temperature in K, and  $F_{reduction}$  (presented in Eq. (2)) is a sigmoidal function of the fuel meat temperature, describing the transition between the two fission rate regimes where the IL growth rate is largely different.

$$F_{reduction} = C_1 \cdot T + \frac{(C_2 - C_1) \cdot T}{1 + \exp(2 \times 10^{-14} \cdot (\dot{f}_{threshold} - \dot{f}))} \quad (2)$$

Here  $\dot{f}_{threshold}$  is the threshold fission rate in fissions/(cm<sup>3</sup>·s), and  $C_1$  and  $C_2$  are constant coefficients listed in table 1 and were fitted to in-pile irradiation results using the DART-2D code [4][5].

Table 1. Parameters in  $F_{reduction}$  fitted for different fuel design\* [4].

Fuel meat composition	Test ID	$\dot{f}_{threshold}$ (fissions/(cm <sup>3</sup> ·s))	$C_1$	$C_2$
U-7wt%Mo / pure Al matrix	FUTURE	$6 \times 10^{14}$	$1 \times 10^{-4}$	$7 \times 10^{-4}$
U-7wt%Mo / Al matrix with Si addition	E-FUTURE	$8 \times 10^{14}$	$1 \times 10^{-4}$	$7 \times 10^{-4}$
Coated U-7wt%Mo particles / pure Al matrix	SELENIUM, SELENIUM-1a	$8 \times 10^{14}$	$1.5 \times 10^{-5}$	$1.05 \times 10^{-4}$

\*Applicability of the parameters depends on reactor operation conditions. For the coated particles, the influence of coating material as well as its thickness was not included in the fitting parameters, which needs further experimental evidences.

It was reasoned in Refs. [4]-[6] that the apparent fission rate effect on IL formation was driven by the variation of activation energy of irradiation-induced interdiffusion in different temperature regimes. However, Correlation I employs a threshold fission rate and a fixed activation energy (0.67 eV), instead of a transition temperature, to describe IL growth transition behavior, because of the lack of direct measurement of fuel temperature during in-pile irradiation and the close correlation between fission rate and fuel temperature in a fuel plate. Ion experiments [7] also indicated that the threshold is rather related to temperature than to fission rate. In spite of the successful representation provided by Correlation I, it is therefore highly desirable to formulate an IL growth correlation manifesting the variation of activation energy over different temperature regimes.

This study is aimed to determine the transition temperature and the activation energies in irradiation-induced U-Mo-Al interdiffusion, using the approach of combining modelling and heavy-ion-irradiation experiments. The planned ion irradiation experiments use high-energy I or Xe ions to bombard Al/U-Mo bi-layer systems at various temperatures and measure the quantity of inter-mixed region in each sample. While the planned heavy-ion-irradiation experiments are still on-going, preliminary results of a new version of IL growth correlation (Correlation II) are obtained using the modelling method and reported here. Upon the completion of heavy-ion-irradiation experiments, the parameters in Correlation II will be verified by comparing with experimental data.

## 2. Experimental data and modeling setting

In-pile irradiation data from seven full-size U-7wt%Mo/Al dispersion plates were employed in this study. Except the AFIP-1T2 plate, which was irradiated in the ATR (USA), all other six plates were irradiated in the BR2 reactor (Belgium). The data selected cover all three types of dispersion fuel design tested: uncoated particles in pure Al matrix, uncoated particles in Al + Si matrix, and Si- or ZrN-coated particles in pure Al matrix. The fabrication characteristics and irradiation conditions of the analyzed plates are listed in Table 2.

Table 2. Fabrication and irradiation characteristics of the analyzed plates.

Test	FUTURE [8]	AFIP-1 [9]	E-FUTURE [8]		SELENIUM [8]		SELENIUM - 1a [3]
Irradiation period	2002-2003	2008-2009	2010-2011		2012		2015-2016
Plate ID	U7MTBR07	1T2	U7MC4202	U7MC6301	U7MD1221	U7MD1231	U7MD1222
Reactor	BR2, Belgium	ATR, USA	BR2, Belgium				
U-Mo powder type	Atomized	Atomized	Atomized	Atomized	Atomized + 600nm Si	Atomized + 1 $\mu$ m ZrN	Atomized + 600nm Si
Mo content (wt%)	7.3	7.0	7.5	7.3	7.2	7.2	7.2
Enrichment (% <sup>235</sup> U)	19.8	19.8	19.8	19.8	19.8	19.8	19.8
Fuel loading (gU/cm <sup>3</sup> )	8.5	8.8	8.1	8.0	8.0	8.0	8.0
Matrix type	Al	Al + 1.9wt%Si	Al + 4.1wt%Si	Al + 6.0wt%Si	Al	Al	Al
Cladding material	AG3NE	Al-6061	AG3NE	AlFeNi	AG3NE	AG3NE	AG3NE
Max. heat flux BOL (W/cm <sup>2</sup> )	351	250	453	472	421	466	278
Total EFPD (days)	40	57	77	77	70	70	98
Plate average burnup (% <sup>235</sup> U)	25		48.1	47.5	47.9	47.5	53.1
Plate average FD (f/cm <sup>3</sup> UMo)	1.8 $\times$ 10 <sup>21</sup>		3.6 $\times$ 10 <sup>21</sup>	3.6 $\times$ 10 <sup>21</sup>	3.5 $\times$ 10 <sup>21</sup>	3.5 $\times$ 10 <sup>21</sup>	4.0 $\times$ 10 <sup>21</sup>
Plate max burnup (% <sup>235</sup> U)	31.9		71.3	71.4	69.2	69.6	73.5
Plate max FD (f/cm <sup>3</sup> UMo)	2.4 $\times$ 10 <sup>21</sup>	3.4 $\times$ 10 <sup>21</sup>	5.5 $\times$ 10 <sup>21</sup>	5.5 $\times$ 10 <sup>21</sup>	5.3 $\times$ 10 <sup>21</sup>	5.3 $\times$ 10 <sup>21</sup>	5.5 $\times$ 10 <sup>21</sup>
Life average fission rate (f/cm <sup>3</sup> UMo/s)	5.2 $\times$ 10 <sup>14</sup>		5.4 $\times$ 10 <sup>14</sup>	5.4 $\times$ 10 <sup>14</sup>	5.8 $\times$ 10 <sup>14</sup>	5.4 $\times$ 10 <sup>14</sup>	4.7 $\times$ 10 <sup>14</sup>

The DART-2D computational code [10] was utilized to fit the parameters in Correlation II. The computation settings include:

- 1) One EFPD (effective full power day) per time step;
- 2) The mesh scheme in the plate length and width directions is identical to the set-up in neutronics calculations;
- 3) Fuel particle size distributions are input.

The input information for the plates irradiated in the BR2 reactor was provided by SCK•CEN, including fabrication characteristics, nominal plate dimensions, coolant conditions, and MCNP-calculated power profiles. Power history of the AFIP-1T2 plate was taken from Ref. [11].

### 3. Construction of Correlation II

During irradiation, the IL thickness increases at each time step and the incremental IL thickness within a time step ( $\Delta Y$ ) is adapted from Refs. [12] and [13].

$$\Delta Y^2 = 2.6 \times 10^{-16} (\dot{f})^{0.5} \cdot \Delta t \cdot \exp\left(-\frac{Q}{2kT}\right) \cdot F_{contact} \quad (3)$$

where  $\Delta Y$  is in cm,  $\dot{f}$  is the fission rate in fissions/(cm<sup>3</sup>·s),  $\Delta t$  is the time interval in s,  $k$  is the Boltzmann constant given by  $k = 8.617 \times 10^{-5}$  eV/K,  $T$  is the fuel meat temperature in K,  $Q$  is the activation energy in eV, and  $F_{contact}$  is an unitless constant between 0 and 1, describing the effective contact surface area between U-Mo particles and the matrix. The details of each parameter (activation energy, transition temperature and  $F_{contact}$ ) in Eq. (3) are described below.

#### 3.1 The activation energy ( $Q$ )

If we assume that the “barrier efficiency” of the diffusion barrier does not evolve significantly with irradiation,  $F_{contact}$  will be a constant for a specific fuel configuration in Eq.(3), and the controlling term of the U-Al mixing rate is the activation energy  $Q$  at a given temperature. Because it has been assessed that the “barrier efficiency” of a ZrN barrier as mostly used in the latest experiments, is mainly dependent on the defects (cracks) in the coating, this is a sound starting point for the system. For the use of Si for IL formation reduction, the “barrier” layer will be amorphous and its properties in terms of diffusion reduction are not expected to evolve dramatically.

The change of activation energy in different temperature regimes accounts for the change of IL growth rate. It is assumed in this study that  $Q$  keeps the same profile for all types of U-7Mo/Al dispersion fuels, since it represents an intrinsic property of fission-enhanced interdiffusion between U-7Mo and Al.  $Q$  is modelled as a sigmoidal function of fuel temperature. The values of its parameters were obtained by fitting to the irradiation data from the FUTURE test, in which the plates have the basic configuration (uncoated U-7Mo particles embedded in a pure Al matrix).

$$Q = 0.78 + \frac{0.1}{1 + \exp(0.05 \times (T - T_{transition}))} \quad (4)$$

where  $T$  is the fuel temperature in K and  $T_{transition}$  is the transition temperature in K. The value of  $T_{transition}$  depends on fuel configuration, which is described in Section 3.2. For the FUTURE test,  $T_{transition} = 400$  K provides the best agreement with the measurement results. Fig. 1 shows the profile of  $Q$  for the FUTURE plates.

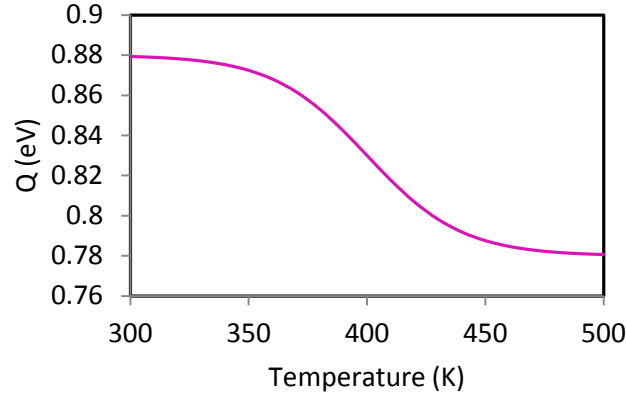


Figure 1. Profile of the activation energy for the system of uncoated U-7Mo particles embedded in an Al matrix.

$Q$  in Eq. (4) varies between 0.78 and 0.88 eV, which is consistent with the results obtained in previous studies. Ref. [13] gives the activation energy of 0.5 to 0.8 eV based on the fitting with U-7Mo/Al mini-plate test data. The slight difference may be due to the different fitting procedure used in the two studies, i.e. time-varied power history in this study vs. time-averaged power in Ref. [13]. Additionally, the activation energy obtained with Xe and Ar irradiation of U/Al bi-layer system is 0.25 eV and 0.57 eV respectively [5], which is in the same order of magnitude as the current result. The quantitative differences can be explained with the different irradiation environment between ion irradiation and reactor irradiation, although the nature of inter-mixing is similar between fission-induced interdiffusion in a fuel plate and ion-mixing in a thin film system (300 nm Al film on U-Mo substrate in Ref. [5]).

### 3.2 The transition temperature ( $T_{transition}$ )

A sharp transition in mixing rate was observed occurring at 300 K in the U/Al bilayer system during Xe mixing [5]. The temperature was explained as the turning point between the ballistic mixing regime (low temperature) and temperature dependent mixing regime (high temperature). In a reactor environment, the entire fuel plate is irradiated at temperatures (330K – 580K) above the critical temperature of 300 K. Hence, very possibly, any place in a fuel plate is irradiated in the temperature dependent mixing regime. If this is the case,  $T_{transition}$  in Eq. (4) does not represent the transition between the ballistic mixing regime and temperature dependent mixing regime. Instead, it is a descriptive parameter standing for the change of mixing rate within a relatively narrow temperature range in the temperature dependent mixing regime. On the other hand, the currently available experimental data cannot exclude the possibility that the temperature of 300 K determined in Ref. [5] does not represent correctly the situation in in-pile-irradiated fuel plates. One major uncertainty lies in the microstructure of U/Al bilayer system. The microstructure of the samples used in the experiments in Ref. [5] may be different from that of U-Mo and Al in fuel plates, for example orthorhombic uranium vs. body-center-cubic uranium. Therefore, the nature of  $T_{transition}$  needs to be verified with the on-going ion irradiation experiments.

The data of the FUTURE test was chosen as the starting point for parameter fitting.  $T_{transition}$  and  $Q$  were fitted simultaneously to obtain the best match between the results calculated with Correlation I and II. After multiple attempts, Eq. (4) with  $T_{transition} = 400\text{K}$  yields the best agreement. The comparison results are plotted in Fig. 2. Note that the activation energy and transition temperature cannot be directly derived from the Arrhenius plot of IL thickness in Fig. 2(a), because each data point in the plot, representing a particular location in the plate, has different power history and fission rate. This is different from the Arrhenius plot obtained from the ion-mixing experiments in Refs. [5] and [6], in which each data point has the same dose and averaged dose rate.

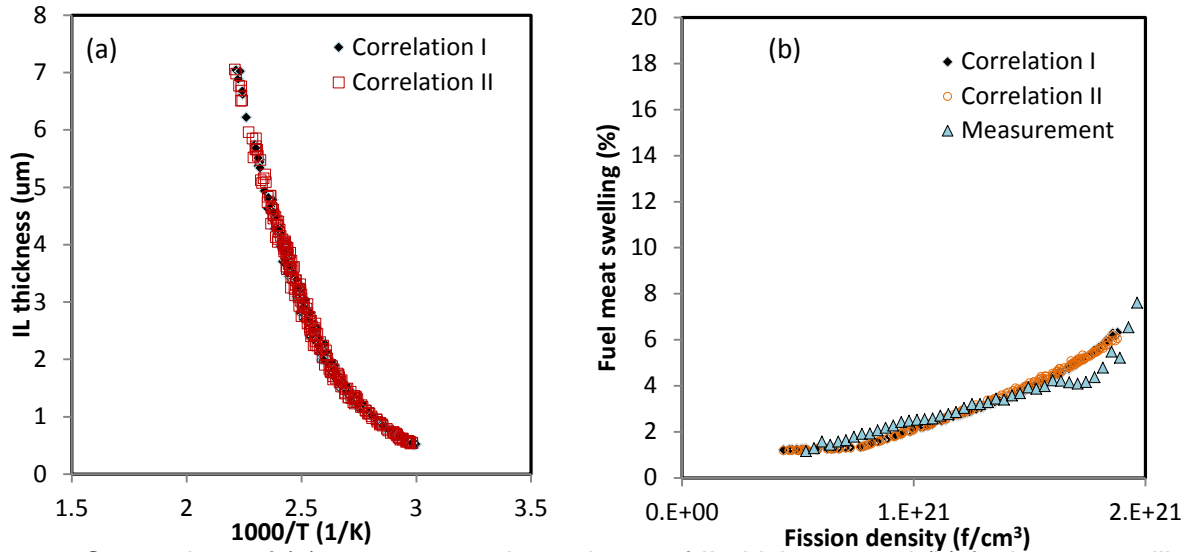


Figure 2. Comparison of (a) temperature dependence of IL thickness and (b) fuel meat swelling in a FUTURE plate at EOL (end-of-life) calculated with Correlation I and II.

Table 3. Transition temperatures for different fuel configuration fitted with DART-2D.

Fuel configuration		$T_{transition}$ (K)	Test data used for fitting
Uncoated U-7Mo particles in an Al-Si matrix	0 wt%Si	400	FUTURE
	2 wt%Si	415	AFIP-1T2
	4 wt%Si	445	EFUTURE-4202
	6 wt%Si	445	EFUTURE-6301
Coated U-7Mo particles in an Al matrix	Si coating	445	SELENIUM-1221 SELENIUM-1222
	ZrN coating	435	SELENIUM-1231

$T_{transition}$  for other fuel configurations were determined using the same approach as what was described for the FUTURE plates. The results are presented in Table 3. For uncoated particle systems, the fitted  $T_{transition}$  increases with the Si content in the Al matrix up to 4 wt% Si and remains the same for the 4 wt% and 6 wt% Si cases. The increase of  $T_{transition}$  with the Si content can be considered as due to elevated energy barrier for interdiffusion between U-7Mo and Al when Si was added into the matrix. Besides the uncertainties involved in the fitting process, the

indistinguishability between the 4 wt% and 6 wt% Si cases is due to two possible reasons. One is that the effect of elevated energy barrier saturates when the Si content reaches 4 wt%, and the other is that the current swelling model in DART-2D does not differentiate the swelling behavior between EFUTURE-4202 and EFUTURE-6301, as DART-2D only simulates the swelling behavior in non-pillowed regions in which the two plates behaved alike, although EFUTURE-6301 has better pillowing behavior than EFUTURE-4202.

In the fuel system containing Si-coated particles, Si coating also increases energy barrier for interdiffusion in the same way as that Si addition in the Al matrix does. Hence, it is plausible for Si-coated fuel system has the same  $T_{transition}$  as that of the uncoated fuel system with 4 wt% or 6 wt% Si in the matrix. The fitting result of  $T_{transition}$  for ZrN-coated particles is slightly lower than that of Si-coated particles, but the difference is not significant with respect to the uncertainties in temperature calculations [4] or/and the measurement error in PIE data. It therefore does not imply that Si coating is superior to ZrN coating in terms of reducing IL formation.

### 3.3 Effective contacting coefficient ( $F_{contact}$ )

$F_{contact}$  was introduced to describe the effective contact surface area between U-Mo particles and the Al matrix. This parameter represents not only the coverage rate of coating on particle surface but also its resistance to irradiation damage. Therefore,  $F_{contact}$  is conceptualized to be a unitless constant that varies between 0 and 1. For perfect blocking,  $F_{contact} = 0$  and there is no IL formation; for the basic fuel system of uncoated U-7Mo/Al (e.g. the FUTURE plates),  $F_{contact} = 1$ . For other fuel systems,  $F_{contact}$  was treated as a variable and fitted together with  $T_{transition}$ . Table 4 lists  $F_{contact}$  for all fuel systems.

Table 4. Effective contacting coefficient for different fuel configuration fitted with DART-2D.

Fuel configuration		$F_{contact}$	Test data used for fitting
Uncoated U-7Mo particles in an Al-Si matrix	0 wt%Si	1.0	FUTURE
	2 wt%Si	1.0	AFIP-1T2
	4 wt%Si	0.9	EFUTURE-4202
	6 wt%Si	0.9	EFUTURE-6301
Coated U-7Mo particles in an Al matrix	Si coating	0.25	SELENIUM-1221
		0.15	SELENIUM-1222
	ZrN coating	0.25	SELENIUM-1231

In reality,  $F_{contact}$  for coated particles is not equal to zero, because the coating layer compromised its function as diffusion barrier during fabrication and irradiation. Coatings were cracked and spalled off by the mechanical wear imposed during rolling, and part of U-Mo particle surface was exposed to the Al matrix [14]. Broken coating is the major cause of IL formation in the SELENIUM plates [1]. Transmission electron microscopy (TEM) investigation of the SELENIUM plates showed that the thickness of coating reduced with burnup for both Si and ZrN coating [15]. At the fission density of  $\sim 5 \times 10^{21}$  f/cm<sup>3</sup>, no pure Si coating or SiRDL (Si-rich

diffusion layer) was found in the sample taken from the plate SELENIUM-1221. Although ZrN coating is still present at this fission density, its thickness reduced to 0.4  $\mu\text{m}$  from the nominal 1  $\mu\text{m}$ , and the Al matrix reacted with ZrN to form Al-ZrN.

As coating degraded more severely in the high fission density regions in the SELENIUM plates [15], it is speculated that coating degradation correlates with fission rate or fuel temperature. Irradiation results of the SELENIUM-1222 plate confirmed this supposition. The SELENIUM-1222 plate, which was identical to the SELENIUM-1221 plate before irradiation, was irradiated to the same burnup as the SELENIUM-1221 plate but at a much lower fission rate [3]. SEM observations of the SELENIUM-1222 plate revealed that the SiRDLs formed between Si coating and U-Mo particles before irradiation remained intact even at  $5.4 \times 10^{21}$  f/cm<sup>3</sup> [3]. In other words, Si coating in the SELENIUM-1222 plate was able to better keep its protective nature than that in the SELENIUM-1221 plate. Accordingly, the SELENIUM-1222 plate has a lower  $F_{\text{contact}}$ . However, the currently available data are too limited to provide a confirmation on whether there is temperature effect involved in coating degradation.

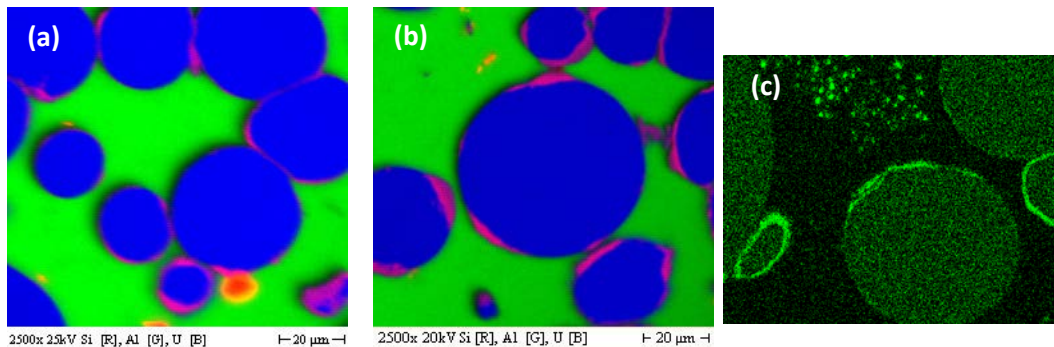


Figure 3. Si X-ray maps of (a) plate E-FUTURE-4201 (4 wt% Si, identical to E-FUTURE 4202), (b) plate E-FUTURE 6311 (6 wt% Si, identical to E-FUTURE 6301) and (c) as-fabricated plate IRIS-3 (2 wt% Si). (images are from Ref. [16]) Color indicators: Al green, U blue and Si red in (a) and (b); Si green in (c).

Although there was no coating applied on the U-7Mo particles in the E-FUTURE plates, a SiRDL formed at the U-Mo-Al interface during fabrication through Si diffusion to U-Mo [16]. This SiRDL helps reduce the Al diffusion to U-Mo particle surface and works in a similar way as Si coating. Therefore,  $F_{\text{contact}}$  for the fuel systems with Si addition is less than 1. Fitting results suggested  $F_{\text{contact}} = 0.9$  for both the 4 wt% and 6 wt% Si addition cases. Its plausibility can be confirmed with the similar SiRDL morphology [16] between the two E-FUTURE plates, shown in Figs. 3 (a) and (b). For the case with 2 wt% Si addition (the AFIP-1T2 data), no fresh fuel characterization result is available. Considering that the IRIS3 plate has similar fabrication parameters as those of AFIP-1T2, their microstructures before irradiation should be close. The SEM micrograph of the as-fabricated IRIS3 plate (Fig. 3(c)) indicated that the coverage and thickness of SiRDLs were much less than the E-FUTURE plates and more small Si particles

remained in the matrix. Therefore, the plate with 2 wt% Si has a higher  $F_{contact}$  than the plate with 4 wt% or 6 wt% Si in the matrix. In this study,  $F_{contact}$  is equal to 1 for the AFIP-1T2 plate.

#### 4. Sensitivity study of the parameters in Correlation II

Sensitivity analyses were performed to evaluate how much the different values of each parameter in Correlation II affect the simulation results of dispersion fuel behavior. The approach adopted in this study is varying one parameter at a time and keeping all other parameter at their optimized values. The sensitivity study results of  $Q$ ,  $T_{transition}$  and  $F_{contact}$  are described below.

##### 4.1 Sensitivity study of $Q$

The optimized  $Q$  is a sigmoidal function of fuel temperature, varying between  $(0.83 - 0.05)$  eV and  $(0.83 + 0.05)$  eV. Both the median and variation range of  $Q$  were subjected to sensitivity study. As  $Q$  was first fitted with the FUTURE data, its parametric study was performed with the FUTURE data as well.

The first variable studied is the variation range of  $Q$ . Variation ranges of  $\pm 0.025$  eV,  $\pm 0.05$  eV and  $\pm 0.075$  eV were applied separately while the median was fixed at 0.83 eV. The results are plotted and compared in Figure 4. All three cases generated very similar results in terms of temperature dependence of IL thickness and fuel meat swelling at EOL.

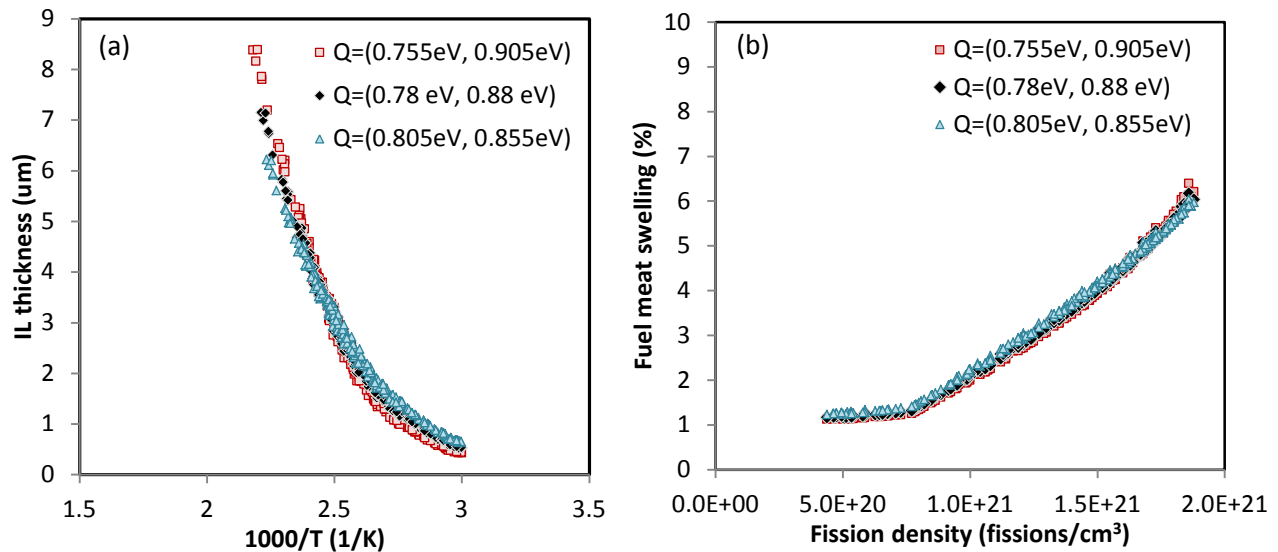


Figure 4. Comparison of (a) Temperature dependence of IL thickness and (b) fuel meat swelling in a FUTURE plate at EOL (end-of-life) when the range of  $Q$  is  $(0.805\text{eV}, 0.855\text{eV})$ ,  $(0.78\text{ eV}, 0.88\text{ eV})$ , and  $(0.755\text{ eV}, 0.905\text{ eV})$ .

The next variable examined is the median of  $Q$ . Three cases were compared:  $(0.53 \pm 0.05)$  eV,  $(0.83 \pm 0.05)$  eV and  $(1.13 \pm 0.05)$  eV. As illustrated in Fig. 5, substantial differences were

inflicted by the variation of the median of  $Q$ . The lower the median of  $Q$ , the higher IL growth rate. Consequently, higher fuel meat swelling and temperature at EOL were obtained with a lower median of  $Q$ . In the case of  $(0.53 \pm 0.05)$  eV, the Al matrix was consumed completely and IL thickness became saturated in regions where fission density is higher than  $8 \times 10^{20}$  fissions/cm<sup>3</sup>. It is also noticed that with the same amount deviation away from the optimized value, a reduced median of  $Q$  affects the results more than that of an elevated median of  $Q$ .

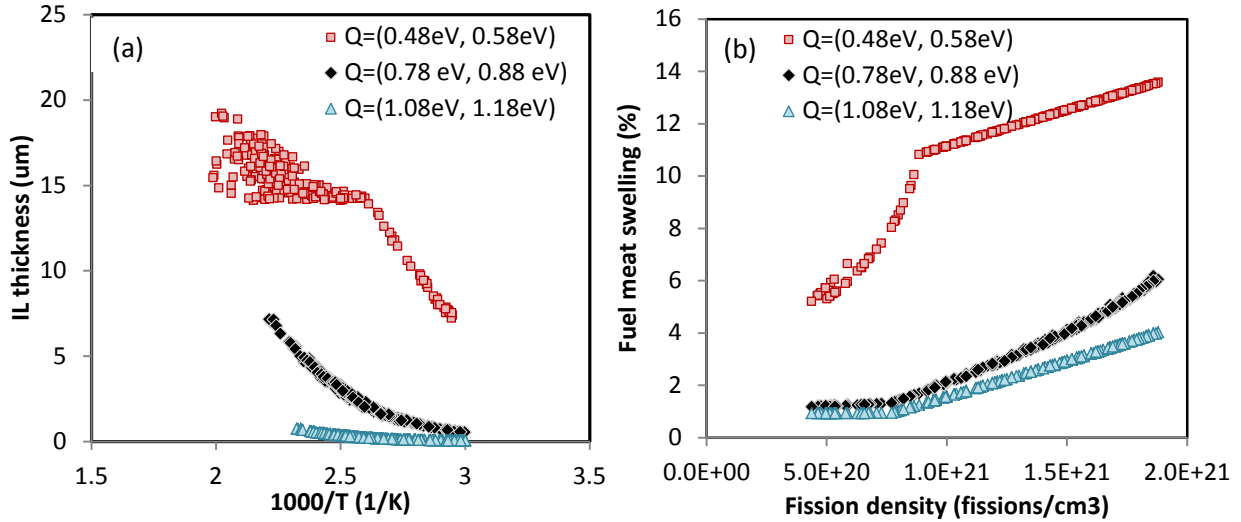


Figure 5. Comparison of (a) Temperature dependence of IL thickness and (b) fuel meat swelling in a FUTURE plate at EOL (end-of-life) when the range of  $Q$  is (0.48eV, 0.58eV), (0.78 eV, 0.88 eV), and (1.08 eV, 1.18 eV).

#### 4.2 Sensitivity study of $T_{transition}$

The FUTURE data is also used as the representative case for the sensitivity study of  $T_{transition}$ . The uncertainty analyses [4] of the temperature calculations in DART-2D showed that the largest temperature uncertainty during a high-power irradiation is around 60 K. Therefore,  $T_{transition}$  was varied +30 K and -30 K away from the optimal value (400 K) for this sensitivity analysis. Fig. 6 shows the comparison of the calculation results at three different transition temperatures: 370 K, 400 K and 430 K. Lowering  $T_{transition}$  promotes IL growth and subsequently fuel meat swelling. The difference in fuel meat swelling at EOL is ~ 2% when  $T_{transition}$  decrease from 430 K to 370 K. This difference will propagate when the calculation is extended to higher burnup.

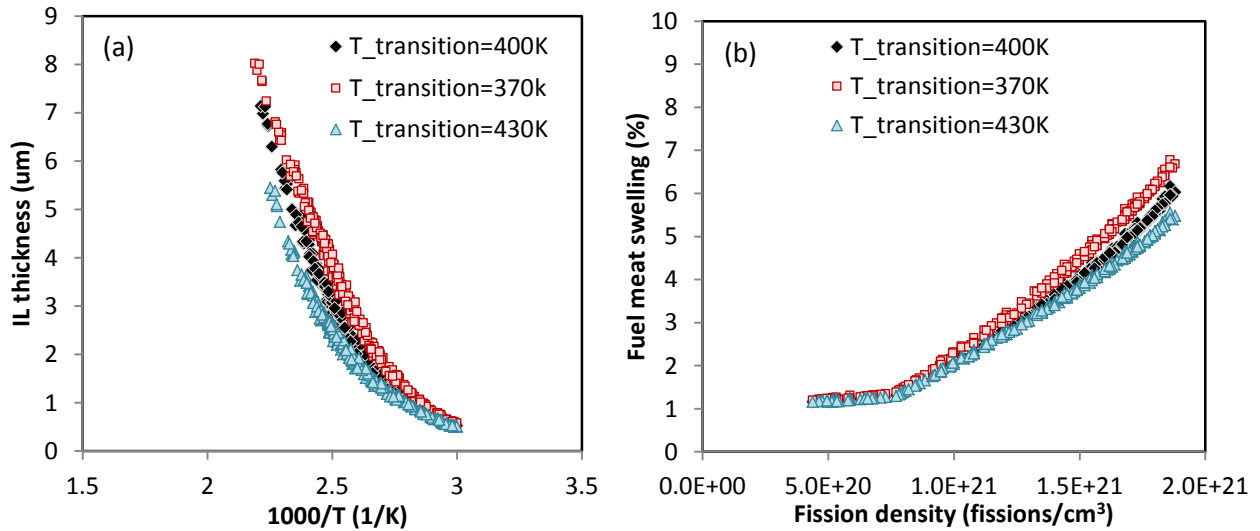


Figure 6. Comparison of (a) Temperature dependence of IL thickness and (b) fuel meat swelling in a FUTURE plate at EOL (end-of-life) when  $T_{transition}$  varies  $\pm 30$  K away from the optimized value.

#### 4.3 Sensitivity study of $F_{contact}$

The data from the SELENIUM-1231 plate was chosen for the sensitivity study of  $F_{contact}$ . This plate contains ZrN-coated U-7Mo particles. According to the definition of  $F_{contact}$  in Section 3.3, the higher  $F_{contact}$ , the weaker coating effectiveness. The effect can be seen in Fig. 7, in which IL thicknesses and fuel meat swelling of three cases calculated with  $F_{contact} = 0.15, 0.25$  and  $0.35$ , respectively, are compared. The differences in results between the cases of  $F_{contact} = 0.15$  and  $0.25$  are more apparent than those between the cases of  $F_{contact} = 0.25$  and  $0.35$ .

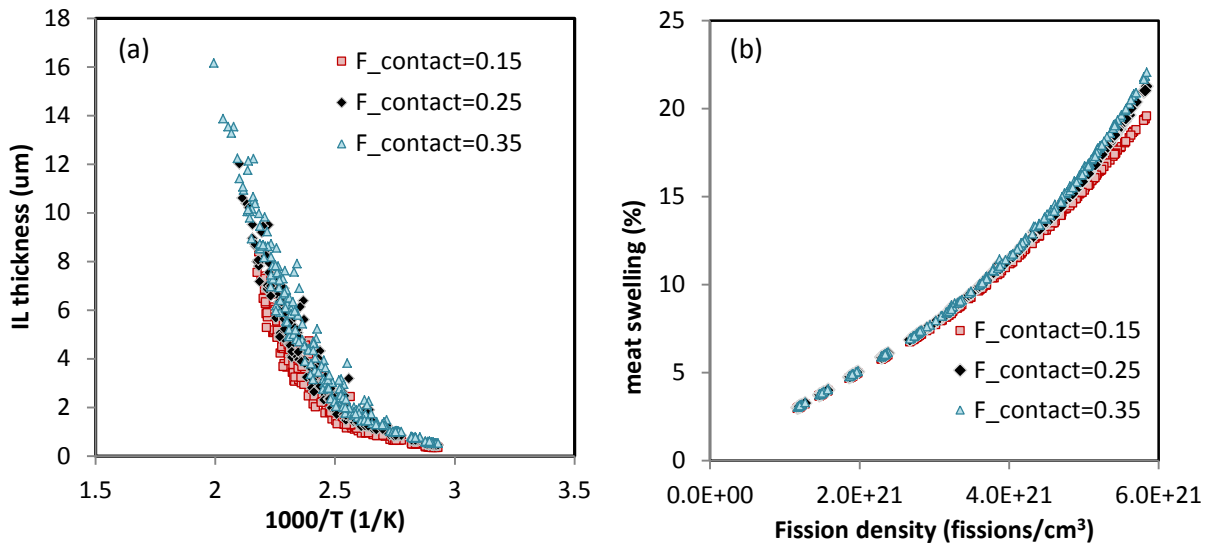


Figure 7. Comparisons of (a) temperature dependence of IL thickness and (b) fuel meat swelling for different  $F_{contact}$  values.

in the SELENIUM-1231 (ZrN-coated) plate at EOL (end-of-life) when  $F_{contact} = 0.15, 0.25$  and  $0.35$ , respectively.

## 5. Conclusions

An IL growth correlation (Correlation II) was formulated with a transition temperature and varied activation energy in different temperature regimes. The efficiency of the diffusion barrier at the U-Mo/Al interfaces was also taken into account. Comparing to Correlation I, which was constructed using a threshold fission rate, Correlation II brings out more underlying mechanisms of the fission-induced IL growth process.

The parameters in the correlation were obtained by fitting to the IL thickness predicted by Correlation I and experimental data using the DART-2D code. Seven sets of experimental data, representing 6 different fuel configurations, were employed for parameter fitting. The activation energy, assumed to be the same for all different U-7 wt%Mo/Al dispersion fuels, is a sigmoidal function varying between 0.78 and 0.88 eV as a function of fuel meat temperature. The transition temperature increases with the Si content in the matrix, from 400 K for a pure Al matrix to 445 K from an Al matrix with 6 wt% Si. The effective contacting coefficient varies between 0 and 1 and is affected by both fabrication condition and irradiation parameters.

Sensitivity studies were performed for activation energy, transition temperature and effective contacting coefficient in Correlation II. The calculation results show that IL growth is more sensitive to the change of the median of activation energy than to that of its variation range. The changes of transition temperature and contacting coefficient impact simulation results as well. However, each individual parameter may have a tolerance range associated with its optimized value, within which the change of the parameter values will have a negligible impact on calculation results. In addition, the current sensitivity study did not explore the effect of simultaneous variation of multiple parameters. Hence, a different combination of parameters may generate the same results. Therefore, the parameters in Correlation II will be assessed with heavy ion irradiation results.

## Acknowledgements

This work was supported by the U.S. Department of Energy, National Nuclear Security Administration (NNSA), Office of Material Management and Minimization (NA-23) Reactor Conversion Program.

This work is supported by the U.S. Department of Energy, Basic Energy Sciences, Office of Science, under contract # DE-AC02-06CH11357. The submitted manuscript has been created by UChicago Argonne, LLC, Operator of Argonne National Laboratory ("Argonne"). Argonne, a U.S. Department of Energy Office of Science laboratory, is operated under Contract No. DE-AC02-06CH11357. The U.S. Government retains for itself, and others acting on its behalf, a paid-up nonexclusive, irrevocable worldwide license in said article to reproduce, prepare derivative works, distribute copies to the public, and perform publicly and display publicly, by or on behalf of the Government.

## References

- [1] A. Leenaers, S. Van den Berghe, E. Koonen, V. Kuzminov, C. Detavernier, J. Nucl. Mater., 458 (2015) 380-393.
- [2] A. Leenaers, S. Van den Berghe, J. Van Eyken, E. Koonen, F. Charollais, P. Lemoine, Y. Calzavara, H. Guyon, C. Jarousse, D. Geslin, D. Wachs, D. Keiser, A. Robinson, G. Hofman, Y.S. Kim, J. Nucl. Mater., 441 (1-3) (2013) 439-448.
- [3] A. Leenaers, Y. Parthoens, G. Cornelis, V. Kuzminov, E. Koonen, S. Van den Berghe, B. Ye, G. Hofman, J. Schulthess, J. Nucl. Mater., 494 (2017) 10-19.
- [4] B. Ye, G.L. Hofman, A. Leenaers, A. Bergeron, V. Kuzminov, S. Van den Berghe, Y.S. Kim, H. Wallin, J. Nucl. Mater., 499 (2018) 191-203.
- [5] François Rossi, M. Nastasi, M. Cohen, C. Olsen, J.R. Tesmer, C. Egert, J. Mater. Res., 6 (6) (1991) 1175-1187.
- [6] R.S. Averbach, Nucl. Instrum. Meth. B, 15, 675 (1986).
- [7] H. Breitzkreutz, J. Hingerl, A. Heldmann, Ch. Steyer, T. Zweifel, R. Jungwirth, J. Shi, W. Petry, in: Proc. Int. Meeting on Reduced Enrichment for Research and Test Reactors (RERTR), Antwerp, Belgium, Oct. 23 - 27, 2016
- [8] S. Van den Berghe, P. Lemoine, Nucl. Eng. Technol., 46 (2014) 125-146.
- [9] D.M. Wachs, A.B. Robinson, F.J. Rice, N.C. Kraft, S.C. Taylor, M. Lillo, N. Woolstenhulme, G.A. Roth, J. Nucl. Mater., 476 (2016) 270-292.
- [10] B. Ye, A. Bergeron, H. Wallin, G. Hofman, Y.S. Kim, A. Leenaers, V. Kuzminov, S. Van den Berghe, in: Proc. Int. Meeting on Reduced Enrichment for Research and Test Reactors (RERTR), Antwerp, Belgium, Oct. 23 - 27, 2016.
- [11] D.M. Perez, M.A. Lillo, G.S. Chang, G.A. Roth, N.E. Woolstenhulme, D.M. Wachs, "AFIP-1 irradiation summary report," INL/EXT-11-22045 (2011).
- [12] Y.S. Kim, G.L. Hofman, H.J. Ryu, J.M. Park, A.B. Robinson, D.M. Wachs, Nucl. Eng. Technol., 45 (2013) 827-838.
- [13] Y.S. Kim, G.L. Hofman, H.J. Ryu, J. Phase Equil. Diff. 27 (2006) 614-621.
- [14] A. Leenaers, S. Van den Berghe, C. Detavernier, J. Nucl. Mater., 440 (2013) 220-228.
- [15] W. Van Renterghem, B.D. Miller, A. Leenaers, S. Van den Berghe, J. Gan, J.W. Madden, D.D. Keiser Jr., J. Nucl. Mater., 498 (2018) 60-70.
- [16] X. Iltis, F. Charollais, M.C. Anselmet, P. Lemoine, A. Leenaers, S. Van den Berghe, E. Koonen, C. Jarousse, D. Geslin, F. Frery, H. Guyon, in: Proceedings of the 32<sup>nd</sup> International Meeting on Reduced Enrichment for Research and Test Reactors (RERTR), Lisbon, Portugal, 2010.